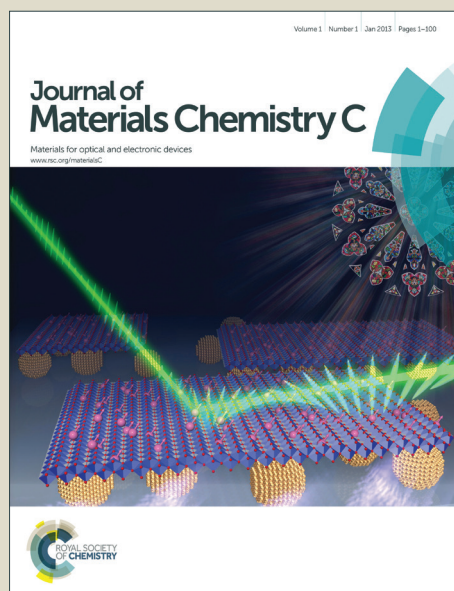


Journal of Materials Chemistry C

Accepted Manuscript



This article can be cited before page numbers have been issued, to do this please use: R. Li, Z. Liu, K. Parvez, X. Feng and K. Muellen, *J. Mater. Chem. C*, 2014, DOI: 10.1039/C4TC02197E.



This is an *Accepted Manuscript*, which has been through the Royal Society of Chemistry peer review process and has been accepted for publication.

Accepted Manuscripts are published online shortly after acceptance, before technical editing, formatting and proof reading. Using this free service, authors can make their results available to the community, in citable form, before we publish the edited article. We will replace this *Accepted Manuscript* with the edited and formatted *Advance Article* as soon as it is available.

You can find more information about *Accepted Manuscripts* in the [Information for Authors](#).

Please note that technical editing may introduce minor changes to the text and/or graphics, which may alter content. The journal's standard [Terms & Conditions](#) and the [Ethical guidelines](#) still apply. In no event shall the Royal Society of Chemistry be held responsible for any errors or omissions in this *Accepted Manuscript* or any consequences arising from the use of any information it contains.

COMMUNICATION

High-Performance Deformable Photoswitches with p-Doped Graphene as Top Window Electrode

Cite this: DOI: 10.1039/C4TC02197E

Rongjin Li,^a Zhaoyang Liu,^a Khaled Parvez,^a Xinliang Feng^{*ab} and Klaus Müllen^{*a}Received 10th January 2012,
Accepted 10th January 2012

DOI: 10.1039/C4TC02197E

www.rsc.org/

Deformable polymer photoswitches with p-doped single layer graphene as top window electrode exhibit excellent photoresponse with on/off ratio as high as 8.5×10^5 . The charge-transfer doping of graphene results in better charge separation and collection efficiency and the structure of top electrode minimizes the dark current.

Photoswitches are widely used for numerous applications, including environmental monitoring, optoelectronic circuits and remote control.¹⁻⁵ For ideal photoswitches, they should exhibit high on/off ratio (ratio of photo current to dark current) and low energy consumption.⁶ To meet the requirements of the next generation organic optoelectronic circuits, they should also be flexible and light-weighted. While optoelectronic devices made of inorganic materials (such as *a*-Si:H) are widely used, they are relatively brittle and heavy. Organic photosensitive polymers are good candidates for constructing flexible polymer photoswitches since they are inherently flexible compared to their inorganic counterparts. Furthermore, they have advantages such as compatibility with low-cost solution processing for large-area detection, a wide selection of materials, and are light-weighted. In general, there are two types of photoswitches based on polymers, i.e. photodiodes in which the photosensitive materials are bulk heterojunction blends of electron donors (D) and acceptors (A) [such as a blend of poly(3-hexylthiophene) (P3HT) and [6,6]-phenyl C₆₁-butyric acid methyl ester (PCBM)], and photoconductors, which are electrically conductive polymers that become more conductive due to the absorption of light radiation. Photodiodes have several advantages over photoconductors, e.g., they are self-powered (working in the photovoltaic mode) and have a reduced electron-hole recombination (formation of a built-in electric field).^{2,7} Photodiodes exhibit a much higher photoresponse speed and higher photosensitivity than photoconductors.⁸

Photodiodes are typically fabricated with a sandwich geometry having two electrodes of different work function (WF) and at least one of them being transparent (the window electrode).^{2,9} The transparent electrode acts as both a window for light to pass through to the photosensitive material and an

Ohmic contact for charge carrier collection. Indium tin oxide (ITO), as the most widely used window electrode material in optoelectronic devices,^{2,3,9-15} is however inherently brittle, which makes it unsuitable for flexible devices. Moreover, ITO is a toxic material with the potential to generate high amounts of reactive oxygen species and is thus a biohazard.¹⁶ Recently, graphene has emerged as an attractive alternative because of its outstanding electronic, optoelectronic, and mechanical properties.¹⁷ Although graphene shows excellent flexibility¹⁸ and high transmittance in the visible range¹⁹ coupled with low sheet resistance (R_s)²⁰, the use of graphene as top window electrode for flexible optoelectronic devices has rarely been investigated.²¹

In this work, we report the first deformable organic polymer photoswitch arrays with p-doped single layer graphene (SLG) as the top window electrode. An electron-withdrawing fluoropolymer, poly(vinylidene fluoride-co-hexafluoropropene) (PVDF-HFP), is used to transfer and simultaneously dope the chemical vapor deposition (CVD)-grown SLG. The p-doping induced by the fluoropolymer not only decreases the R_s , but also increases the WF of graphene for better charge separation and collection. Photoswitches were fabricated using p-doped SLG as the top window electrode, which avoids the deposition of metal on the photosensitive polymer and minimizes the dark current. Remarkably, the fabricated photoswitches show a high on/off ratio up to 8.5×10^5 , which is the highest value for organic photoswitches reported so far^{6,7}, indicating the excellent performance of the device. Moreover, the fabricated photoswitches with graphene anode are flexible and can be bent or even crumpled, demonstrating their high potential in stretchable electronics.²²

Single layer graphene was produced by chemical vapor deposition on a copper foil and transferred to the target substrates by thin poly(methyl methacrylate) (PMMA, denoted hereafter as G) or PVDF-HFP (denoted hereafter as FG) film. PVDF-HFP was selected as the p-dopant due to its electron-deficient nature, excellent film formation property and high tensile strength.²³ Inorganic substances such as AuCl₃ or HNO₃ were commonly used as p-dopant for graphene. However, doping by these materials was unstable due to either the hygroscopic effect or the volatile nature of the dopant.^{24,25} In contrast, PVDF-HFP doped graphene films are stable and the

COMMUNICATION

change of R_s are less than 5% over a period of 2 month (Figure S1, Supporting Information).

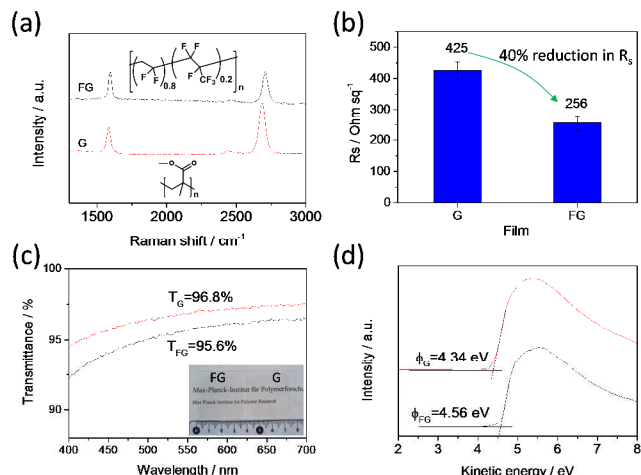


Fig. 1 (a) Raman spectra (the inset shows the chemical structure of PVDF-HFP and PMMA), (b) sheet resistance, (c) transmittance, and (d) UPS spectra of G and FG film on polyethylene naphthalate (PEN) substrate.

Raman spectroscopy was firstly employed to investigate the electronic structure of both graphene films. Compared to G, FG exhibited a marked decrease of the intensity ratio of the 2D to G peak (I_{2D}/I_G) from 3.4 to 1.9, and a decrease of the full-width at half maximum of the G band from 33.3 to 27.2 cm^{-1} in the Raman spectra.²⁶ The blue shift of both the G and 2D frequencies (9.5 and 20.5 cm^{-1} for the G and 2D peaks, respectively) further confirmed the p-doping effect (Figure 1a).^{26,27} The doping was ascribed to the dipoles formed at the interface as a consequence of electron transfer from the π -bonding levels of graphene near the Dirac point to the lowest unoccupied molecular orbital (LUMO) of the dopant (PVDF-HFP).^{28–32} Based on the shift of the G peak (9.5 cm^{-1}), a decrease of the Fermi level of ~ 0.2 eV is estimated.²⁷ Due to the effective p-doping (i.e., the move of the Fermi level away from the Dirac point), the R_s significantly decreased from 425 Ωsq^{-1} (G) to 256 Ωsq^{-1} (FG, $\sim 40\%$ reduction, Figure 1b). Nevertheless, the transmittance of the FG was decreased by only 1.2% compared to that of the G (Figure 1c). Moreover, the work function of G film determined by ultraviolet photoelectron spectroscopy (UPS) was 4.34 eV and this value increased to 4.56 eV after doping (Figure 1d). Considering that graphene is a zero-gap semiconductor, the increase of work function (0.21 eV) coincides with the decrease of Fermi level determined by Raman spectroscopy (~ 0.2 eV). The decreased R_s and increased WF render FG a good candidate as anode for the fabrication of photoswitches.

Encouraged by the enhanced electronic properties of FG, we next applied the graphene films as the window electrode for the fabrication of flexible photoswitches. The main procedures are shown in Figure S2 (Supporting Information). First, SLG on Cu foil was patterned with a shadow mask using a previously described method³³ (Figure S2a–2b). Subsequently, PVDF-HFP or PMMA solution was spin-coated on the pattern and the Cu foil was etched away using a $\text{Fe}(\text{NO}_3)_3$ aqueous solution (Figure S2c). Al bottom electrodes (60 nm thick) were deposited onto polyethylene naphthalate (PEN) or polyethylene terephthalate (PET) substrates with the same shadow mask and the photosensitive polymer layer (blend of P3HT:PCBM) was spin-coated on top of the Al bottom electrodes (Figure S2d–2e). Finally, PVDF-HFP or PMMA-supported graphene patterns were positioned on top of the PEN or PET substrate and vertically aligned with the bottom Al electrodes

(Figure S2f). Thus, photoswitches with 8×8 arrays were built up with a sandwich structure of substrate/Al/P3HT:PCBM/SLG (Figure 2a). Figure 2b–2c shows photographs of the devices in the flat state and being bent.

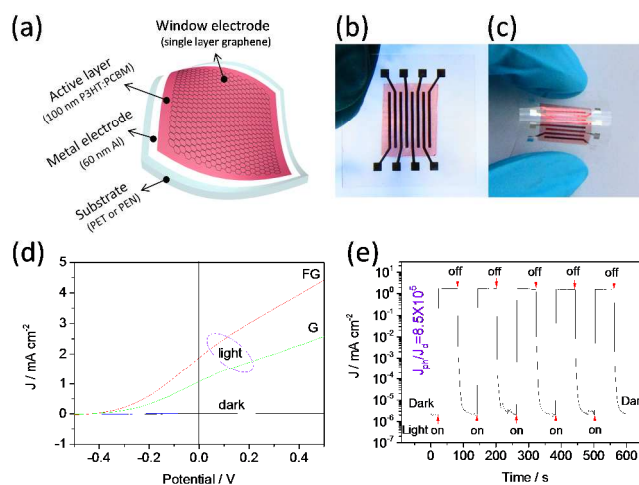


Fig. 2 Schematic structure and photoresponse of photoswitches based on G and FG top window electrodes. (a) Sketch of the structure of the photoswitches with graphene as the top window electrode. (b–c) Photographs of the photoswitches in the flat state and being bent. (c) J–V characteristics of G-photoswitch and FG-photoswitch. (d) Photoresponse of FG-photoswitch.

Typical current–voltage (J–V) characteristics of the photoswitches with G (G-photoswitch) and FG (FG-photoswitch) as the top window electrode are presented in Figure 2d. The curves moved far away from the origin (0,0), which is indicative of photovoltaic effect.³⁴ Both G-photoswitch and FG-photoswitch had a similar open-circuit voltage (V_{OC}) of ~ 0.44 V. Remarkably, FG-photoswitch exhibited a short-circuit current (J_{SC}) of 1.9 mA cm^{-2} , which was 72% higher than that of G-photoswitch (1.1 mA cm^{-2}). The increased J_{SC} was ascribed to the increased WF and decreased R_s of FG, which facilitated charge separation and collection. Taking advantage of the photovoltaic effect, the FG-photoswitches could work at 0 V bias, meaning that photons could be detected without an external energy supply. Figure 2e shows the photoresponse of FG-photoswitches at 0 V bias. The current density of the devices was lower than 10^{-5} mA cm^{-2} in the dark, whereas it jumped sharply by more than five orders of magnitude upon light irradiation (ca. 20 mW cm^{-2}). When the light was switched on and off, the devices responded to the light and exhibited two states: a “high” current state under illumination (J_{ph}) and a “low” current state in the dark (J_d). Thus, an on/off ratio (J_{ph}/J_d) as high as 8.5×10^5 was achieved. By comparison, G-photoswitch exhibited a lower on/off ratio of 1.2×10^5 (Figure S3, Supporting Information).

The prominent photoresponse behaviour of FG-photoswitches can be ascribed to two primary features. First, the use of FG anode results in high charge separation efficiency, and thus high photocurrent (J_{ph}). By p-doping, the increased WF of the anode results in a larger built-in electric field (determined by the WF difference between the anode and cathode), which is more efficient for the separation of photoinduced charges at the D–A interface.³⁵ Without a built-in field, there will be no incentive for the carriers to drift and electrons and holes dissociated at the D–A interfaces would diffuse. When a built-in electric field is formed, the separated charge carriers will move directionally, with electrons move to the cathode and holes move to the anode. The increased WF of the anode (from

G to FG) will create a larger built-in electric field (Figure 3a-3b), thus higher efficiency for charge separation. Moreover, the increased WF of FG results in better alignment of the anode work function with respect to the donor. To form a desired Ohmic contact and effectively collect holes at the anode, the WF of the anode must be approximately equal to the HOMO of the donor. With FG as the anode, the WF is closer to the HOMO of P3HT (5.0 eV) than that of G (4.34 eV) and thus a better hole collection efficiency is expected. Second, the dark current (J_d) is reduced by using transferred top graphene electrode. The device has a structure of substrate/Al/P3HT:PCBM/FG. The FG window electrode is transferred on top of the photosensitive polymer, thus the direct deposition of metal on the polymer layer is avoided. For comparison, we also fabricated devices with a structure of substrate/FG/P3HT:PCBM/Al, in which the Al layer was thermally evaporated on top of the polymer layer. The dark current of such device was on the order of 10^{-3} mA cm $^{-2}$ (Figure 3c), which was nearly three orders of magnitude higher than that with graphene as the top electrode. Although the photocurrent increased (3.6 fold), the on/off ratio decreased to 4.4×10^3 (Figure 3c-3d). The increased dark current can be attributed to the diffusion of metal atoms into the polymer layer, which tends to form clusters on or below the surface of the polymer.³⁶⁻³⁸

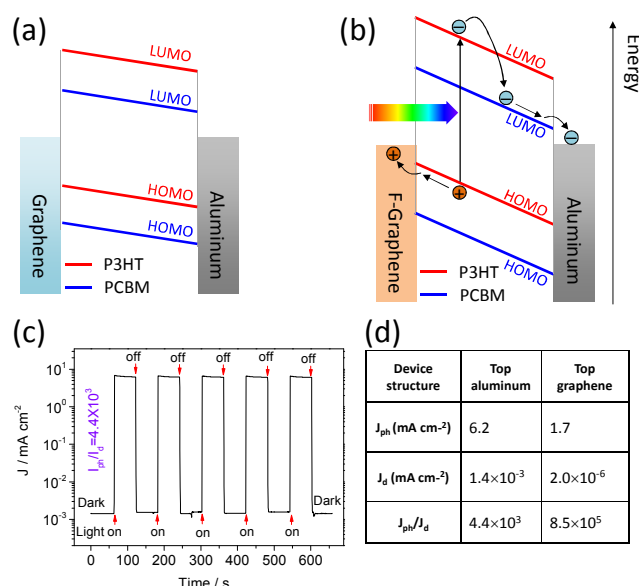


Fig. 3 (a-b) Simple energy level diagrams of the photoswitches using G or FG as the window electrode in the short circuit mode. (c) Photoresponse of devices with evaporated aluminium as the top electrode. (d) Comparison of the photoresponse of photoswitches with both top graphene and top aluminium electrodes.

We further examined the bendability of the photoswitches with p-doped graphene as top window electrode. Even after 900 cycles of repeated bending of the FG-photoswitches (on 175- μ m thick PEN film) to a radius of ~ 6 mm, there was little change in the photoresponse (Figure S4, Supporting Information). For applications in wearable electronics, the devices need to be both bendable and deformable.²² Thus, we also fabricated FG-Photoswitches on 2.5- μ m thick PET films to afford devices with a total thickness of less than 2.7 μ m. The ultrathin devices were lightweight (1.6 mg for an 8 \times 8 array) and exhibited extremely good flexibility. To further evaluate the photoresponse stability after deformation, the devices were

crumpled into a ball of ~ 5 mm in diameter and then flattened (Figure 4a-4c). The radius of curvature of the wrinkles was estimated to be several tens of micrometers (Figure 4d). Remarkably, the devices could still perform as photoswitches and the photoresponse behaviour was only slightly changed (Figure 5e). The mean on/off ratio of nine randomly selected devices was decreased by less than 10% after the deformation (Figure S5, Supporting Information), highlighting the outstanding flexibility of the photoswitches and their robustness to mechanical deformation.

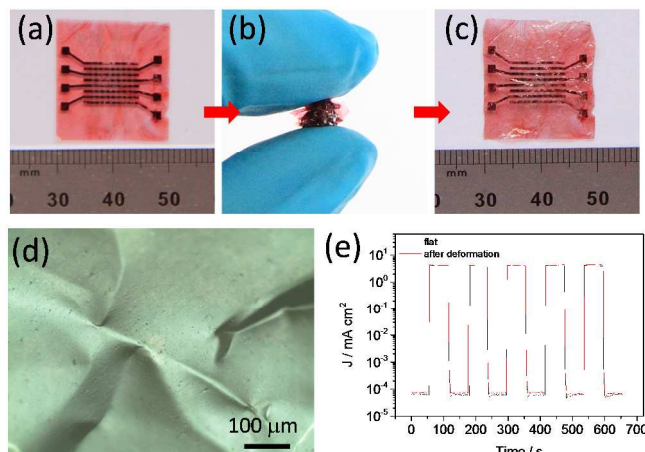


Fig. 4 Deformable photoswitches. (a-c) Photographs of a flat, crumpled, and flattened device. (d) Optical micrograph of the PET surface of the photoswitch before crumpled and flattened. (e) A typical photoresponse curve before and after deformation.

Conclusions

In summary, we developed the first deformable polymer photoswitch arrays with PVDF-HFP doped SLG as top window electrode. The introduction of p-doped graphene facilitated the charge separation and collection, and the structure of the transferred top window electrode avoided the diffusion of metal into the polymer and minimized the dark current. This resulted in high on/off ratio of 8.5×10^5 . The device structure developed in this study provides an inexpensive but efficient method of fabricating high-performance flexible photoswitches as well as other ITO-free flexible optoelectronic devices, such as organic light-emitting diodes or organic photovoltaic cells.

Acknowledgements

This work was financially supported by ERC grants on NANOGRAPH and 2DMATER, DFG Priority Program SPP 1459, EU Projects GENIUS, UPGRADE and MoQuaS, EC under Graphene Flagship (No. CNECT-ICT-604391), and support from Cfaed of TU Dresden. The authors thank Dr. Ye Zou (Institute of Chemistry, Chinese Academy of Sciences) for the XPS and UPS measurements.

Notes and references

^a Max Planck Institute for Polymer Research

Ackermannweg 10, Mainz 55128, Germany

Tel, +49 6131 379 150, Fax, +49 6131 379 350

E-mail: feng@mpip-mainz.mpg.de, muellen@mpip-mainz.mpg.de

^b Technische Universitaet Dresden

01062 Dresden, Germany

Tel, +49 351 463 43250

† Electronic Supplementary Information (ESI) available. See

DOI: 10.1039/c000000x/

- 1 H. Dong, H. Zhu, Q. Meng, X. Gong and W. Hu, *Chem. Soc. Rev.* 2012, **41**, 1754.
- 2 G. Konstantatos and E. H. Sargent, *Nat Nano* 2010, **5**, 391.
- 3 X. Gong, M. Tong, Y. Xia, W. Cai, J. S. Moon, Y. Cao, G. Yu, C.-L. Shieh, B. Nilsson and A. J. Heeger, *Science* 2009, **325**, 1665.
- 4 Q. X. Tang, L. Q. Li, Y. B. Song, Y. L. Liu, H. X. Li, W. Xu, Y. Q. Liu, W. P. Hu and D. B. Zhu, *Adv. Mater.* 2007, **19**, 2624.
- 5 G. Konstantatos, I. Howard, A. Fischer, S. Hoogland, J. Clifford, E. Klem, L. Levina and E. H. Sargent, *Nature* 2006, **442**, 180.
- 6 H. Zhu, T. Li, Y. Zhang, H. Dong, J. Song, H. Zhao, Z. Wei, W. Xu, W. Hu and Z. Bo, *Adv. Mater.* 2010, **22**, 1645.
- 7 S. Pang, S. Yang, X. Feng and K. Müllen, *Adv. Mater.* 2012, **24**, 1566.
- 8 L. Peng, L. Hu and X. Fang, *Adv. Mater.* 2013, **25**, 5321.
- 9 T. Rauch, M. Boberl, S. F. Tedde, J. Furst, M. V. Kovalenko, G. Hesser, U. Lemmer, W. Heiss and O. Hayden, *Nat. Photon.* 2009, **3**, 332.
- 10 G. Yu, J. Wang, J. McElvain and A. J. Heeger, *Adv. Mater.* 1998, **10**, 1431.
- 11 P. Peumans, V. Bulovic and S. R. Forrest, *Appl. Phys. Lett.* 2000, **76**, 3855.
- 12 Y. Yao, Y. Liang, V. Shrotriya, S. Xiao, L. Yu and Y. Yang, *Adv. Mater.* 2007, **19**, 3979.
- 13 X. Gong, M.-H. Tong, S. H. Park, M. Liu, A. Jen and A. J. Heeger, *Sensors* 2010, **10**, 6488.
- 14 F. Guo, B. Yang, Y. Yuan, Z. Xiao, Q. Dong, Y. Bi and J. Huang, *Nat. Nanotech.* 2012, **7**, 798.
- 15 F. Guo, Z. Xiao and J. Huang, *Adv. Opt. Mater.* 2013, **1**, 289.
- 16 D. Lison, J. Laloy, I. Corazzari, J. Muller, V. Rabolli, N. Panin, F. Huaux, I. Fenoglio and B. Fubini, *Toxicol. Sci.* 2009, **108**, 472.
- 17 A. K. Geim and K. S. Novoselov, *Nat. Mater.* 2007, **6**, 183.
- 18 K. S. Kim, Y. Zhao, H. Jang, S. Y. Lee, J. M. Kim, J. H. Ahn, P. Kim, J. Y. Choi and B. H. Hong, *Nature* 2009, **457**, 706.
- 19 F. Bonaccorso, Z. Sun, T. Hasan and A. C. Ferrari, *Nat. Photon.* 2010, **4**, 611.
- 20 S. Bae, H. Kim, Y. Lee, X. Xu, J.-S. Park, Y. Zheng, J. Balakrishnan, T. Lei, H. Ri Kim, Y. I. Song, Y.-J. Kim, K. S. Kim, B. Ozyilmaz, J.-H. Ahn, B. H. Hong and S. Iijima, *Nature Nanotech.* 2010, **5**, 574.
- 21 Z. Liu, J. Li and F. Yan, *Adv. Mater.* 2013, **25**, 4296.
- 22 T. Someya: *Stretchable Electronics* Wiley-VCH: Weinheim, Germany, 2013.
- 23 K. H. Lee, M. S. Kang, S. Zhang, Y. Gu, T. P. Lodge and C. D. Frisbie, *Adv. Mater.* 2012, **24**, 4457.
- 24 I. H. Lee, U. J. Kim, H. B. Son, S.-M. Yoon, F. Yao, W. J. Yu, D. L. Duong, J.-Y. Choi, J. M. Kim, E. H. Lee and Y. H. Lee, *J. Phys. Chem. C* 2010, **114**, 11618.
- 25 G. Jo, M. Choe, S. Lee, W. Park, Y. H. Kahng and T. Lee, *Nanotechnology* 2012, **23**, 112001.
- 26 X. Dong, D. Fu, W. Fang, Y. Shi, P. Chen and L.-J. Li, *Small* 2009, **5**, 1422.
- 27 DasA, PisanaS, ChakrabortyB, PiscanecS, S. K. Saha, U. V. Waghmare, K. S. Novoselov, H. R. Krishnamurthy, A. K. Geim, A. C. Ferrari and A. K. Sood, *Nat. Nanotech.* 2008, **3**, 210.
- 28 W. Chen, S. Chen, D. C. Qi, X. Y. Gao and A. T. S. Wee, *J. Am. Chem. Soc.* 2007, **129**, 10418.
- 29 T. Wehling, K. Novoselov, S. Morozov, E. Vdovin, M. Katsnelson, A. Geim and A. Lichtenstein, *Nano Lett.* 2008, **8**, 173.
- 30 H. Pinto, R. Jones, J. P. Goss and P. R. Briddon, *J. Phys.: Condens. Matter* 2009, **21**, 402001.
- 31 H. Medina, Y.-C. Lin, D. Obergfell and P.-W. Chiu, *Adv. Funct. Mater.* 2011, **21**, 2687.
- 32 A. C. Crowther, A. Ghassaei, N. Jung and L. E. Brus, *ACS Nano* 2012, **6**, 1865.
- 33 S. P. Pang, H. N. Tsao, X. L. Feng and K. Müllen, *Adv. Mater.* 2009, **21**, 3488.
- 34 S. J. Fonash: *Solar Cell Device Physics (Second Edition)*; Academic Press: Burlington, USA, 2010.
- 35 A. W. Hains, Z. Liang, M. A. Woodhouse and B. A. Gregg, *Chem. Rev.* 2010, **110**, 6689.
- 36 F. Faupel, R. Willecke and A. Thran, *Mater. Sci. Eng., R* 1998, **22**, 1.
- 37 J. Zhu, P. Goetsch, N. Ruzycski and C. T. Campbell, *J. Am. Chem. Soc.* 2007, **129**, 6432.
- 38 F. Bebensee, J. Zhu, J. H. Baricatro, J. A. Farmer, Y. Bai, H.-P. Steinrück, C. T. Campbell and J. M. Gottfried, *Langmuir* 2010, **26**, 9632.

TOC:

Deformable polymer photoswitches with p-doped single layer graphene as the top window electrode exhibit an on/off ratio as high as 8.5×10^5 .

